JOURNAL OF AIRCRAFT
Vol. 35, No. 6, November–December 1998

Free Vibration of Thick Generally Laminated Quadrilateral Plates Having Arbitrarily Located Point Supports

Rakesh K. Kapania* and Andrew E. Lovejoy†
Virginia Polytechnic Institute and State University, Blacksburg, Virginia 24061-0203

Free vibration of generally laminated plates having arbitrarily located point supports is studied via the Rayleigh–Ritz method. Chebychev polynomials are chosen as the trial functions and essential boundary conditions along the edges are imposed by means of appropriate large artificial springs. This allows for the edges of the plate to be free, simply supported, or clamped. An elastically restrained point is represented by the appropriate spring constant value and by allowing this spring constant to become large, a point support is represented. The first-order shear deformation theory is utilized in the development of the equations of motion, along with the linear stress/strain relationship. Verification of the method is carried out through comparison with published results for point-supported plates. After the method is verified, a brief study of generally laminated plates having point supports is carried out. The method developed is simple and efficient, making it perfectly suited to applications that require multiple calculations, such as optimization, and can be applied to analyze joined-wings and truss-braced wings.

Introduction

POINT-supported and elastically restrained plates find many applications. For example, in civil engineering, bridge and building spans can be considered as point-supported plates. Similarly, circuit boards used in electronics can also be considered as point-supported plates. However, the authors are motivated by the potential of the present method as applied to aircraft structures, namely, joined-wing and trussed-braced wing components. A great deal of focus has been directed at the analysis of isotropic point-supported plates, but point-supported plates of composite construction have received little attention.

Thin isotropic plates with point supports have received a great deal of attention in the literature,[1–16] and Mizusawa and Kajita[14] present a significant review of the literature available until 1987. Recent works regarding point supports include those of Bhat,[1] Gorman,[4] Bapat and Suryanarayan,[6–8] and Bapat et al.[9] Edge supports are included in some of the references,[6–9,11–14] the most recent of which is that of Saliba.[12] Thick isotropic square and skew plates with point supports were studied by Aksu and Felemban[15] and Kitipornchai et al.,[16] respectively. Orthotropic plates with point supports were studied by Srinivasan and Munaswamy.[17] However, plates of composite construction with point supports have not been so widely studied. One such reference found by the authors dealing with these plates is that of Sadasiva Rao and Singh.[18] In that paper, the authors investigate corner-supported, square, thick plates using the finite element method. Several uses of plates having point supports can be found in civil engineering applications, such as bridge sections. However, the authors are motivated by recent studies on the designs of joined-wing aircraft,[19,20] and of truss-braced aircraft.[21] The truss-braced aircraft is being proposed to increase the aspect ratio of the wings of future large transports.[21] The attachment point of the tail horizontal section to the main wing of joined-wing aircraft and the truss attachment point for truss-braced aircraft can be represented by an elastically restrained point, thus allowing for the analysis of individual components.

The Rayleigh–Ritz procedure has been applied by Lovejoy and Kapania[22–24] in the analysis of quadrilateral, thick, generally laminated plates having arbitrary edge supports. Chebychev polynomials are taken as the trial functions. Using laminate shear correction factors of $k_4 = k_5 = \sqrt{\pi^2/12}$, the first-order shear deformation theory is implemented (for an isotropic plate the shear correction factor is $\kappa = (k_4)^2$). This method is the basis for the present research, which is intended to give some insight into the analysis and behavior of laminated plates having arbitrarily placed elastically restrained and fixed point supports, and having any combination of free, simply supported, and clamped edges. Although these types of plates can be analyzed using the finite element method, at times it is more beneficial to have a method that is computationally simple and that still yields accurate results.

Theory

The procedure employed by Lovejoy and Kapania[22–24] is utilized and expanded. Figure 1 shows the plate definition and transformed coordinates. The familiar related transformation equations for this mapping are given by

$$x = \sum_{i=1}^{4} N_i(\eta, \xi)x_i, \qquad y = \sum_{i=1}^{4} N_i(\eta, \xi)y_i \tag{1}$$

where

$$\begin{aligned} N &= \tfrac{1}{4}(1 + \eta)(1 - \xi), \qquad N_2 = \tfrac{1}{4}(1 + \eta)(1 + \xi) \\ N_3 &= \tfrac{1}{4}(1 - \eta)(1 + \xi), \qquad N_4 = \tfrac{1}{4}(1 - \eta)(1 - \xi) \end{aligned} \tag{2}$$

and x_i and y_i are the corner coordinates of the plate defined in Fig. 1. The determinant for the Jacobian, $|J|$, as needed for evaluating the integrals is easily found. Transverse shear is

Presented as Paper 96-1346 at the AIAA/ASME/ASCE/ASC 37th Structures, Structural Dynamics, and Materials Conference, Salt Lake City, UT, April 15–17, 1996; received June 18, 1996; revision received Jan. 28, 1998; accepted for publication June 24, 1998.

*Professor, Department of Aerospace and Ocean Engineering. Associate Fellow AIAA.

†Graduate Research Assistant, Department of Aerospace and Ocean Engineering; currently Research Scientist, Analytical Services and Materials, Inc., 107 Research Drive, Hampton, VA 23666. Member AIAA.

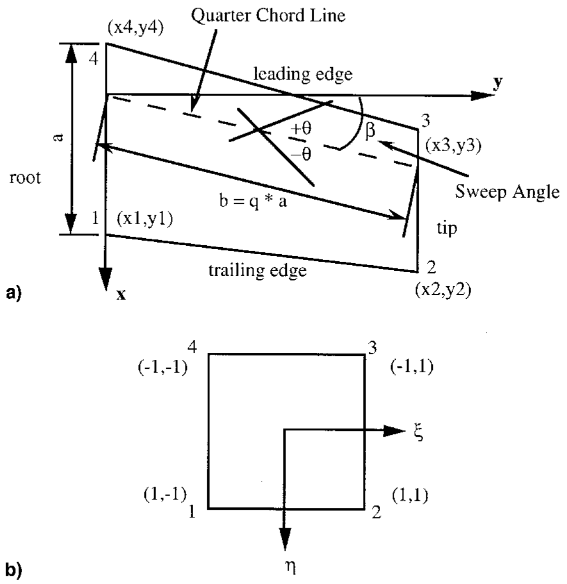

Fig. 1 Plate definition and transformation: a) original and b) transformed coordinates.

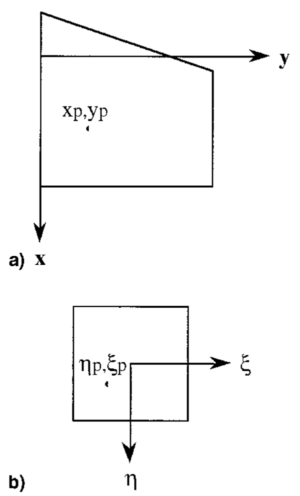

Fig. 2 Elastically restrained or fixed point position in the a) original plate and b) transformed coordinate systems.

included by means of the first-order shear deformation theory (FSDT), with the displacement equations given as

$$u = u^0(x, y, t) + z\phi_x(x, y, t)$$
$$v = v^0(x, y, t) + z\phi_y(x, y, t), \qquad w = w^0(x, y, t) \tag{3}$$

where the superscript denotes midplane quantities. Applying the Rayleigh–Ritz method, each displacement quantity in Eq. (3) is expanded in a series of Chebychev polynomials in the transformed coordinates. The double-series expansions consist of products of the one-dimensional Chebychev polynomials, and are

$$u^0 = \sum_{i=0}^{I}\sum_{j=0}^{J} R_{ij}(t)T_i(\eta)T_j(\xi), \qquad v^0 = \sum_{k=0}^{K}\sum_{l=0}^{L} S_{kl}(t)T_k(\eta)T_l(\xi)$$

$$w^0 = \sum_{m=0}^{M}\sum_{n=0}^{N} P_{mn}(t)T_m(\eta)T_n(\xi) \tag{4}$$

$$\phi_x = \sum_{p=0}^{P}\sum_{q=0}^{Q} X_{pq}(t)T_p(\eta)T_q(\xi), \qquad \phi_y = \sum_{r=0}^{R}\sum_{s=0}^{S} Y_{rs}(t)T_r(\eta)T_s(\xi)$$

where R_{ij}, S_{kl}, P_{mn}, X_{pq}, and Y_{rs} are the time-dependent Rayleigh–Ritz coefficients.

The equations of motion are developed using Lagrange's equations, resulting in the development of the total stiffness and mass matrices, denoted by $[K]$ and $[M]$, respectively. The total stiffness matrix is derived from the potential energy, and is composed of matrices representing the contributions from the strain energy, edge boundary conditions, and elastically restrained and fixed point supports. Thus

$$[K] = [K_{\text{strain}}] + [K_{\text{edges}}] + [K_{\text{pts}}] \tag{5}$$

Linear strain-displacement relations are used, resulting in the stiffness matrix because of strain, given by

$$[K_{\text{strain}}] = \int_{-1}^{1}\int_{-1}^{1} [C]^T[T]^T \left[\begin{array}{cc|c} A & B & \\ B & D & 0 \\ \hline \multicolumn{2}{c|}{0} & A' \end{array}\right] [T][C]|J|\, d\eta\, d\xi \tag{6}$$

Details of the transformation matrix, $[T]$, and the $[C]$ matrix can be found in Ref. 22. The 3×3 submatrices $[A]$, $[B]$, and $[D]$ are associated with the classical laminate theory (CLT) contributions. FSDT contributions are introduced through the 2×2 submatrix given by

$$[A'] = \begin{bmatrix} k_4^2A_{44} & k_4k_5A_{45} \\ k_4k_5A_{45} & k_5^2A_{55} \end{bmatrix} \tag{7}$$

Simply supported and clamped conditions are approximated by large stiffness, linear, and rotational springs applied at the edges. Simply supported edges require $\mu_n^0 = w^0 = \gamma_t = 0$, where μ_n^0 is the midplane displacement normal to the edge, and γ_t is the rotation tangent to the edge. Clamped edges have $\mu_n^0 = \mu_t^0 = w^0 = \gamma_n = \gamma_t = 0$, where μ_t^0 is the midplane displacement tangent to the edge, and γ_n is the rotation normal to the edge. An expression for the potential energy of the edge supports is easily found,[22] leading to a stiffness matrix having the form

$$[K_{\text{edges}}] = \int_{-1}^{1} \begin{bmatrix} K_{11} & 0 & 0 & 0 & 0 \\ 0 & K_{22} & 0 & 0 & 0 \\ 0 & 0 & K_{33} & 0 & 0 \\ 0 & 0 & 0 & K_{44} & 0 \\ 0 & 0 & 0 & 0 & K_{55} \end{bmatrix} d\gamma \tag{8}$$

where details of the submatrices can be found in Refs. 22 and 23.

Point supports and elastic restraints are now introduced by means of linear springs that restrain the transverse deflection, w, for comparison with the references. In the current method, only the transverse deflection is restrained, but additional linear and rotational springs are easily added as desired to restrain the other degrees of freedom. The locations of point supports in the transformed domain are found using the numerical reverse transformation procedure presented by Murti and Valliappan.[25] A numerical reverse transformation is necessary because for the general case, no analytic reverse transformation exists. Figure 2 shows the location of a point in the original and transformed spaces.

The potential energy resulting from a point support is given by

$$\tfrac{1}{2}\alpha w^2(\eta_p, \xi_p) \tag{9}$$

where α represents the linear spring stiffness value, and the subscript p denotes coordinates at the point location. The stiffness matrix resulting from the potential energy associated with the point supports has the form

$$[K_{\text{pts}}] = \begin{bmatrix} 0 & 0 & 0 & 0 & 0 \\ 0 & 0 & 0 & 0 & 0 \\ 0 & 0 & 0 & 0 & 0 \\ 0 & 0 & 0 & 0 & 0 \\ 0 & 0 & 0 & 0 & K_{w_{\text{pts}}} \end{bmatrix} \tag{10}$$

Table 1 Frequency parameter, $\Omega = \omega a^2\sqrt{\rho h/D}$, for an isotropic, thin, square, corner-supported plate, $\nu = 0.3$

Gorman[2]	Raju and Amba-Rao[5]	Gorman[4]	Present study
7.180	7.1018	7.112	7.1104
15.56	15.540	15.55	15.779
19.22	19.220	19.22	19.589
38.36	38.176	38.18	38.400
44.28	44.040	44.08	44.380
50.00	49.824	49.92	50.345
68.12	68.110	68.12	69.234
80.20	80.030	80.08	80.375
91.80	91.460	91.56	92.961
115.1	115.20	115.1	118.93

Table 2 Frequency parameter, $\Omega = \omega a^2\sqrt{\rho h/D}$, for an isotropic, thin, square plate point-supported on the diagonal, $\nu = 0.3$[a]

α/a	Gorman[2]	Raju and Amba-Rao[5]	Gorman[4]	Present study
0.1	12.81	12.810	12.81	12.811
	19.22	19.220	19.22	19.589
	23.39	23.387	23.39	23.795
	54.00	54.009	54.04	54.927
	58.32	58.300	58.32	58.600
0.2	19.22	19.220	19.22	19.589
	23.12	23.121	23.12	23.053
	31.77	31.771	31.77	32.521
	47.36	47.380	47.36	48.554
	——	51.087	51.04	53.330
0.3	19.22	19.220	19.22	19.310
	19.26	19.268	19.26	19.589
	23.58	23.600	23.58	24.659
	——	25.396	25.38	26.405
	36.36	36.355	36.36	37.352

[a]Using terminology of Raja and Amba-Rao.[5]

Table 3 Frequency parameter, $\Omega = \omega a^2\sqrt{\rho h/D}$, for an isotropic, thin, skew, corner-supported plate, $b/a = 1$, $\nu = 0.3$

β	Srinivasan and Munaswamy[17]	Mizusawa and Kajita[14]	Present study
15	7.65	7.583	7.582
	13.29	13.17	13.18
	19.94	19.59	19.60
	20.40	20.29	20.29
	34.41	33.97	33.96
30	9.40	9.104	9.104
	11.89	11.40	11.41
	22.80	22.65	22.65
	26.75	25.18	25.17
	31.54	30.29	30.29
45	11.66	10.21	10.21
	13.21	11.82	11.82
	28.09	27.76	27.78
	32.85	29.78	29.79
	38.32	33.34	33.35

Table 4 Frequency parameter, $\Omega = \omega a^2\sqrt{\rho h/D}$, for an isotropic, thick, skew, corner-supported plate, $\nu = 0.3$

b/a	β	h/a	Kitipornchai, et al.[16]	Present study
1.0	15	0.1	7.0202	7.0853
			11.901	12.011
			16.965	17.149
		0.2	6.1399	6.2227
			10.128	10.230
			13.679	13.794
	30	0.1	8.2609	8.3355
			10.477	10.553
			21.270	21.461
		0.2	7.0469	7.1362
			9.0860	9.1842
			16.538	16.645
	45	0.1	9.5153	9.5697
			10.489	10.570
			25.740	25.787
		0.2	8.3724	8.4727
			8.6833	8.7827
			20.353	20.438
2.0	15	0.1	2.4003	2.4095
			5.7865	5.8564
			8.8392	8.9453
		0.2	2.3075	2.3202
			5.2496	5.3141
			7.7901	7.8790
	30	0.1	2.7892	2.8010
			5.1282	5.1729
			10.705	10.812
		0.2	2.6470	2.6625
			4.7098	4.7572
			9.5785	9.7244
	45	0.1	3.5688	3.5863
			4.6614	4.6875
			9.9525	10.026
		0.2	3.3201	3.3416
			4.3140	4.3507
			8.9853	9.1096

Table 5 Frequency parameter, $\Omega = \omega a^2\sqrt{\rho h/D}$, for an isotropic, thin, cantilever, plate, $\nu = 0.3$[a]

b/a	Narita[11]	Present study
1	8.509	8.5346
	12.13	12.230
	25.61	25.636
	30.96	30.985
	40.23	40.836
2	3.576	3.6429
	3.721	3.7891
	10.93	10.999
	12.15	12.074
	19.54	19.562

[a]With point support at the center of the free edge opposite the clamped edge.

Including any of the other displacements or rotations for a point support will result in the appropriate, additional submatrices along the diagonal.

The mass matrix is derived from the kinetic energy, and is found to be

$$[M] = \int_{-1}^{1}\int_{-1}^{1} \{[Z]^T[\rho_\Psi][Z]\}\,|J|\,d\eta\,d\xi \tag{11}$$

where the matrix $[\rho_\Psi]$ contains the inertia terms defined by

$$\rho_1 = \int_{-h/2}^{h/2} \rho_k\,dz, \quad \rho_2 = \int_{-h/2}^{h/2} \rho_k z\,dz, \quad \rho_3 = \int_{-h/2}^{h/2} \rho_k z^2\,dz \tag{12}$$

Table 6 Frequency hertz, for cantilever plates with point supports at the free corners[a]

Stacking sequence	β	Three-node triangular finite element	Present study
$[45/-45/0]_s$	0	93.490	93.105
		148.32	147.67
		178.18	177.19
		332.97	331.42
		373.56	370.79
	30	80.316	79.960
		159.13	158.93
		170.20	169.99
		247.42	246.56
		409.30	408.39
	45	63.484	63.636
		134.85	136.59
		167.94	168.62
		217.64	218.23
		320.03	325.08
[0.22.5]	0	64.514	64.373
		140.65	139.52
		188.15	187.17
		247.33	246.14
		270.13	269.72
	30	60.533	60.304
		129.59	128.88
		172.50	172.12
		222.39	221.48
		293.76	293.11
	45	54.100	53.816
		128.92	128.85
		143.59	143.65
		176.72	175.86
		276.42	275.72

[a]Compared with results using the three-node finite element of Kapania and Mohan.[26] Laminated plates made from boron/epoxy having aspect ratio = 1, taper ratio = 1, area = 412.9024 cm², and thickness = 0.124968 cm.

and ρ is the mass density. Details for the matrix $[Z]$ are given in Ref. 22.

Natural frequencies are determined from the resulting eigenvalue problem having the form

$$[K - \lambda M]\{q\} = 0 \tag{13}$$

$$\{q\} = \{R_{00}, R_{01}, \ldots, R_{IJ}, S_{00}, \ldots, S_{KL}, X_{00}, \ldots, X_{PQ}, Y_{00}, \ldots, Y_{RS}, P_{00}, \ldots, P_{MN}\}^T \tag{14}$$

where $\lambda = \omega^2$ is an eigenvalue of the system, and ω is the corresponding frequency in radians/second, and $\{q\}$ is the associated eigenvector of Rayleigh–Ritz coefficients.

A Fortran program was developed to perform the natural frequency calculations. As in Refs. 22–24, eight terms are taken in each series unless otherwise indicated, and an eight-point Gaussian quadrature is used for evaluating the integrals. The resulting eigenvalue problem having 320 degrees of freedom is solved using the International Mathematical and Statistical Library subroutine DGVCSP, which uses an algorithm exploiting the symmetry of the stiffness and mass matrices and the positive definiteness of the mass matrix.

Results and Discussion

Verification of Present Method

Isotropic, Point Supports

Comparison of the present method with the references for isotropic plates having only point support can be seen in Tables 1–4. The frequency parameter $\Omega = \omega a^2\sqrt{\rho h/D}$ is utilized, where a is the root length indicated in Fig. 1, h is the total plate thickness, and $D = Eh^3/12(1 - \nu^2)$ is the plate flexural

Table 7 Frequency parameter, $\Omega = (\omega a^2/h)\sqrt{\rho/E_2}$, for symmetrically laminated $[\theta/-\theta/0]_s$, thin, corner-supported plates, $h/a = 0.01$, $b/a = 1$

	β			
θ	0	15	30	45
0	2.727	2.905	3.546	5.117
	5.622	5.763	6.270	7.350
	9.474	10.14	12.36	16.71
	14.79	14.72	15.24	16.99
	16.75	18.28	22.50	29.69
15	2.927	3.109	3.793	5.453
	9.744	9.096	9.020	9.436
	11.74	12.91	15.93	20.31
	19.27	18.69	18.96	22.23
	23.86	25.37	29.12	34.85
30	4.104	4.259	5.157	7.181
	14.18	12.74	11.40	10.17
	16.95	19.34	22.03	23.63
	19.20	20.86	24.92	32.67
	27.89	27.77	30.71	37.24
45	7.610	7.747	8.532	7.849
	10.23	13.16	10.09	9.584
	16.45	13.25	19.39	24.22
	22.22	24.41	27.62	31.69
	38.74	32.35	28.02	32.39
60	5.413	7.348	7.906	6.104
	14.85	10.87	10.15	9.717
	17.30	15.83	16.67	24.18
	20.08	23.51	24.22	24.55
	32.47	27.37	24.45	26.45
75	4.321	5.119	6.389	5.306
	10.47	8.108	7.128	8.627
	14.67	17.28	14.64	16.64
	21.31	20.22	22.71	21.64
	26.81	27.41	26.00	26.06
90	4.038	4.169	4.711	4.383
	6.559	5.752	4.841	5.864
	12.04	14.57	12.89	12.86
	19.47	14.92	19.01	18.73
	19.64	26.93	26.90	22.99

Table 8 Frequency parameter, $\Omega = (\omega a^2/h)\sqrt{\rho/E_2}$, for unsymmetrically laminated $[\theta/-\theta]$, thin, corner-supported plates, $h/a = 0.01$, $b/a = 1$

	β			
θ	0	15	30	45
15	2.800	2.985	3.644	5.220
	7.560	7.488	7.563	7.951
	9.434	10.27	12.76	16.36
	14.62	14.65	15.06	17.57
	17.99	18.87	21.12	24.32
30	3.445	3.668	4.436	6.093
	10.57	9.701	8.741	7.838
	11.16	11.81	13.83	17.20
	11.23	12.65	15.53	20.55
	21.44	22.22	22.28	22.53
45	4.579	4.937	5.870	5.766
	7.916	9.160	7.434	7.008
	12.09	9.708	12.55	18.14
	12.09	14.27	16.91	18.55
	26.73	23.49	19.42	20.82
60	3.445	4.203	5.491	4.175
	10.57	7.723	5.922	6.534
	11.16	11.46	11.53	14.14
	11.23	14.06	15.97	16.38
	21.44	19.36	17.45	20.28
75	2.800	3.279	4.377	3.528
	7.560	5.814	4.609	5.669
	9.434	12.21	9.909	10.84
	14.62	12.63	15.12	14.23
	17.99	19.24	19.88	19.83

Table 9 Frequency parameter, $\Omega = (\omega a^2/h)\sqrt{\rho/E_2}$, for symmetrically laminated $[\theta/-\theta/0]_s$, thick, corner-supported plates, $h/a = 0.1$, $b/a = 1$

	β			
θ	0	15	30	45
0	2.581	2.729	3.242	4.397
	5.038	5.133	5.457	6.079
	7.816	8.231	9.546	12.06
	12.69	12.03	11.97	12.58
	12.86	14.43	17.41	21.90
15	2.745	2.902	3.465	4.719
	7.558	7.153	7.077	7.307
	8.953	9.760	11.51	14.57
	13.78	13.71	13.97	14.87
	16.73	17.26	19.19	22.57
30	3.617	3.757	4.417	5.752
	9.359	8.603	8.026	7.604
	11.06	12.15	13.99	17.10
	12.15	13.09	14.84	17.18
	20.62	19.54	19.21	20.61
45	5.345	5.556	6.064	6.447
	9.568	8.710	7.480	6.813
	10.04	10.87	14.30	17.53
	11.45	12.80	14.72	17.83
	22.59	20.24	18.47	20.00
60	4.470	5.290	6.460	5.380
	9.660	7.921	6.491	7.065
	11.26	12.93	13.68	15.08
	13.23	12.94	14.66	17.02
	21.44	19.11	18.42	21.18
75	3.821	4.301	5.475	4.776
	8.051	6.687	5.544	6.651
	10.07	12.25	12.52	13.18
	15.46	13.79	14.54	16.53
	18.46	18.19	17.80	18.57
90	3.620	3.651	4.075	4.044
	5.850	5.230	4.443	5.025
	9.066	10.15	11.41	11.42
	14.97	12.67	13.30	15.70
	15.62	17.32	16.91	15.76

Table 10 Frequency parameter, $\Omega = (\omega a^2/h)\sqrt{\rho/E_2}$, for unsymmetrically laminated $[\theta/-\theta]$, thick, corner-supported plates, $h/a = 0.1$, $b/a = 1$

	β			
θ	0	15	30	45
15	2.640	2.795	3.330	4.508
	6.356	6.297	6.322	6.544
	7.764	8.318	9.882	12.67
	11.88	11.90	12.20	13.12
	14.54	15.13	16.65	18.74
30	3.137	3.318	3.917	5.089
	7.976	7.445	6.887	6.435
	8.521	9.403	11.14	14.02
	9.750	10.22	11.69	14.27
	17.22	16.86	16.37	16.66
45	3.884	4.114	4.748	5.094
	7.575	7.370	6.124	5.584
	8.670	8.494	11.02	13.87
	8.670	10.00	11.72	14.40
	18.53	17.03	15.19	15.90
60	3.137	3.640	4.763	3.889
	7.976	6.325	4.863	5.409
	8.521	10.00	10.18	11.29
	9.747	10.11	11.69	13.16
	17.22	15.45	14.79	16.88
75	2.640	3.005	3.999	3.334
	6.356	5.135	4.034	4.923
	7.764	9.614	8.979	9.466
	11.88	10.48	11.66	12.34
	14.54	14.99	15.24	15.61

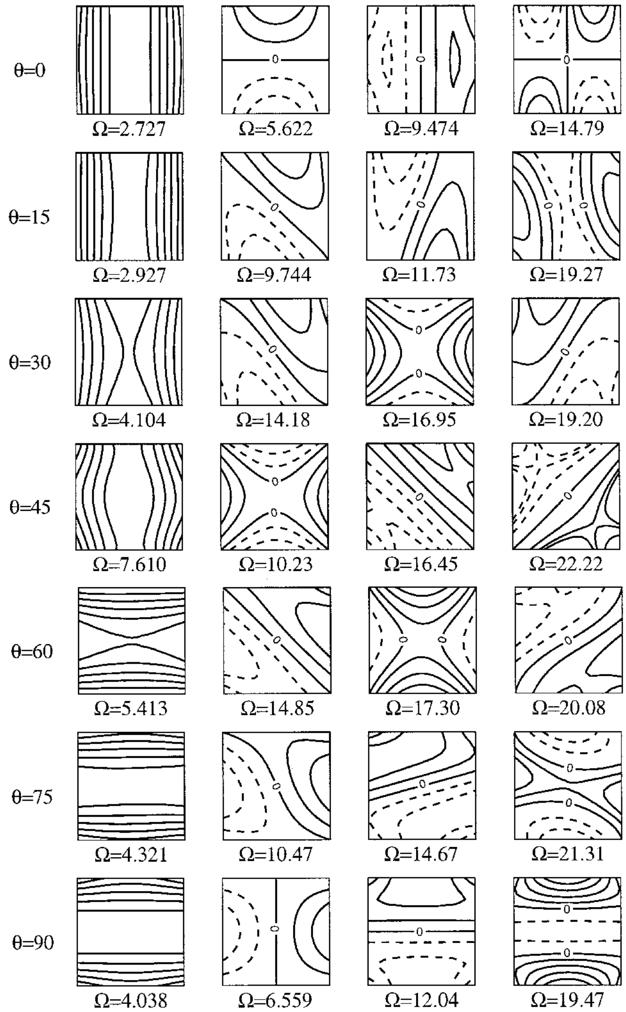

Fig. 3 Frequency parameter, $\Omega = (\omega a^2/h)\sqrt{\rho/E_2}$, for symmetrically laminated $[\theta/-\theta/0]_s$, thin, corner-supported plates, $h/a = 0.01$, $b/a = 1$, $\beta = 0$.

rigidity. Table 1 shows the results for a square, thin isotropic plate that has point supports at the corners. In the references, one-quarter of the plate is analyzed, resulting in the need to impose the boundary conditions necessary to represent a line of symmetry or antisymmetry. This leads to a need to solve the problem three different times to obtain all of the necessary frequencies. Also, this approach is not applicable for unsymmetrically laminated plates. Using the global Rayleigh–Ritz method has eliminated this need in the present study while still yielding accurate results.

Results for a thin, isotropic plate having point supports on the diagonals are presented in Table 2. Skew, thin, isotropic plates having corner point supports are compared in Table 3, and thick, isotropic, skew plates are presented in Table 4 for ratios of $b/a = 1$ and $b/a = 2$. All results in Tables 1–4 show excellent agreement between the references and the present method.

Isotropic, Edge and Point Supports

To further verify the present method, it is applied to plates having edge supports as well as the point supports. Table 5 presents the results for thin, cantilever plates having a single point support in the middle of the free edge opposite the clamped edge. Again, the present method shows excellent agreement when compared with available results.[11]

Laminated, Edge and Point Supports

Lastly, comparison of the present method to previously unavailable results for cantilever laminated plates with point sup-

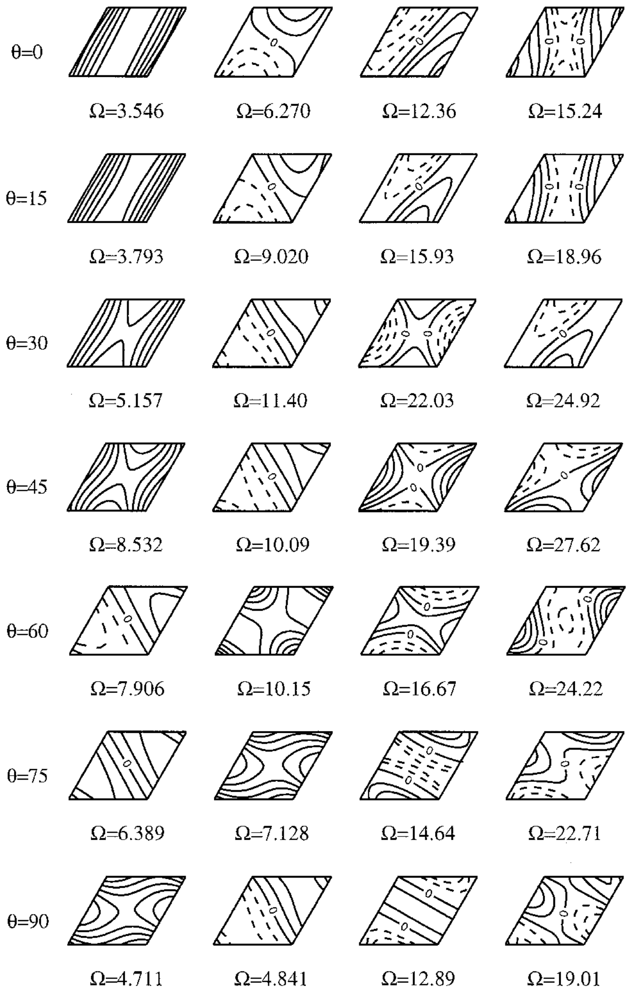

Fig. 4 Frequency parameter, $\Omega = (\omega a^2/h)\sqrt{\rho/E_2}$, for symmetrically laminated $[\theta/-\theta/0]_s$, thin, corner-supported plates, h/a = 0.01, b/a = 1, b/a = 1, β = 30.

ports at the corners has been carried out. The comparative results are found using the three-node shell element developed by Kapania and Mohan.[26] This shell element is a combination of the Allman triangular membrane element and the DKT bending element with a resulting 18-degree-of-freedom element, six at each node. The plates are composed of boron/epoxy with the following properties: E_1 = 161.21 GPa, E_2 = E_3 = 12.52 GPa, G_{12} = G_{13} = 6.75 GPa, G_{23} = 5.47 GPa (calculated letting $G_{23} = 0.81G_{12}$), ν_{12} = 0.22, and ρ = 1881.81 kg/m^3. Table 6 shows the results for thin symmetrically and unsymmetrically laminated plates. Frequencies are given in hertz, and excellent agreement is seen between the two methods.

Square, Point Supported, Laminated Plates

Using the method developed, a brief study of square, corner-supported, generally laminated plates is made. Results are presented to demonstrate the present method and to provide comparative data for future work. The frequency parameter, $\Omega = (\omega a^2/h)\sqrt{\rho/E_2}$, for thin, laminated plate results are given in Tables 7 and 8. E_2 is the Young's modulus in the 2-direction in the material axes. Results are given for symmetric and unsymmetric laminates, respectively. Similarly, results for thick laminated plates are presented in Tables 9 and 10. In each case, the plates are made from graphite/epoxy with property ratios that are given as (Refs. 21–23) E_1/E_2 = 40, G_{12}/E_2 = G_{13}/E_2 = 0.6, G_{23}/E_2 = 0.5, and ν_{12} = 0.25.

Figures 3–6 provide mode shapes and the associated frequency parameters for thin laminated plates. The plots for mode shapes are oriented such that the x axis is at the bottom

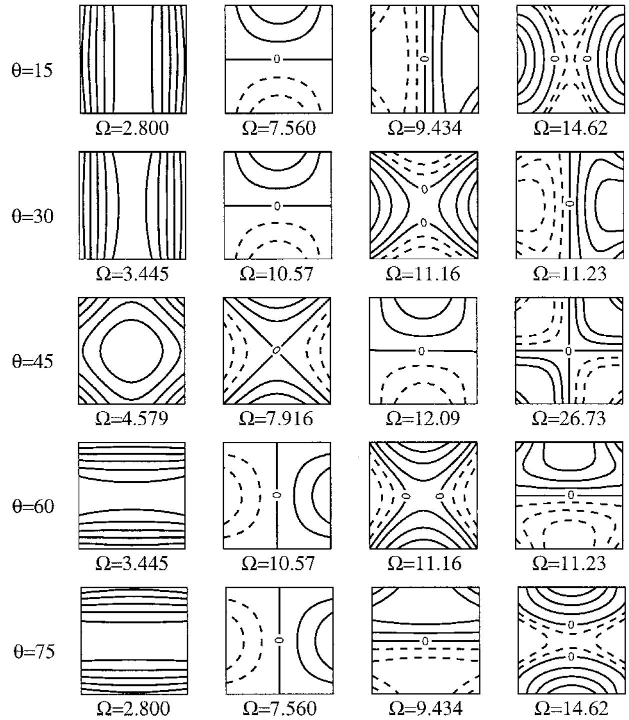

Fig. 5 Frequency parameter, $\Omega = (\omega a^2/h)\sqrt{\rho/E_2}$, for unsymmetrically laminated $[\theta/-\theta]$, thin, corner-supported plates, h/a = 0.01, b/a = 1, β = 0 (for θ = 45, the fourth frequency is a repeated frequency and is omitted).

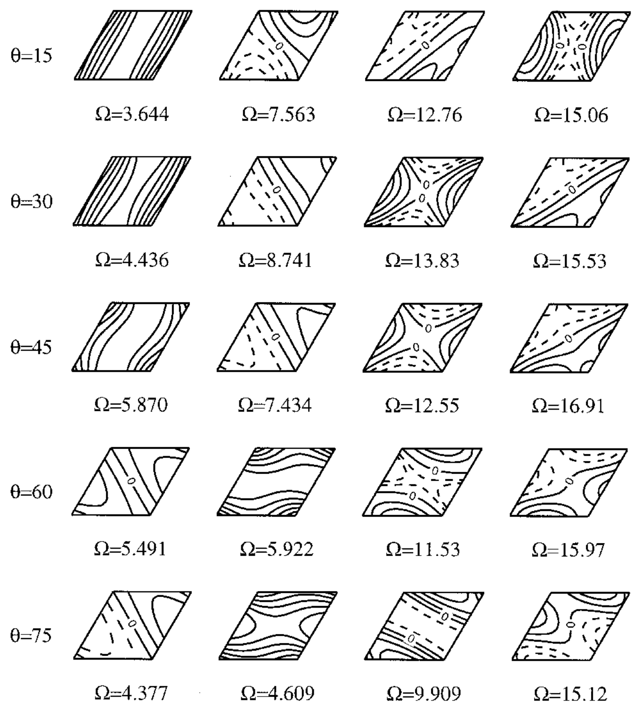

Fig. 6 Frequency parameter, $\Omega = (\omega a^2/h)\sqrt{\rho/E_2}$, for unsymmetrically laminated $[\theta/-\theta]$, thin, corner-supported plates, h/a = 0.01, b/a = 1, β = 30.

of the figure and oriented pointing toward the right, with the y axis oriented pointing up. A study of these figures shows several instances of crossover of mode shapes. For example, Fig. 4 shows that the first and second mode shapes switch for θ between 45 and 60 deg, then again for θ between 75 and 90 deg. Only corner supports are used for the plates of Tables 7–10 and Figs. 3–6, but the point supports can be arbitrarily placed at any number of locations.

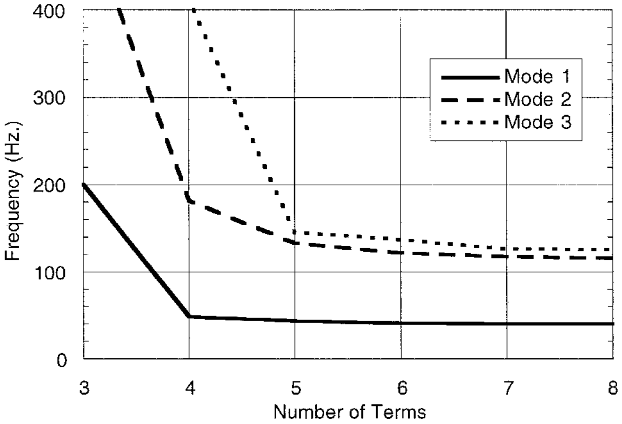

Fig. 7 Frequency in hertz as a function of the number of terms in the series for a symmetrically laminated $[30_2/0]_s$ cantilever plate having a point support at the corner intersection of the tip and trailing edges. The plate is made of glass/epoxy with plate geometry parameters as follows: β = 30, thickness = 0.14 in. (3.556 mm), aspect ratio = 3.11, taper ratio = 0.5, and area = 63.0 in.^{2} (406.45 cm^2).

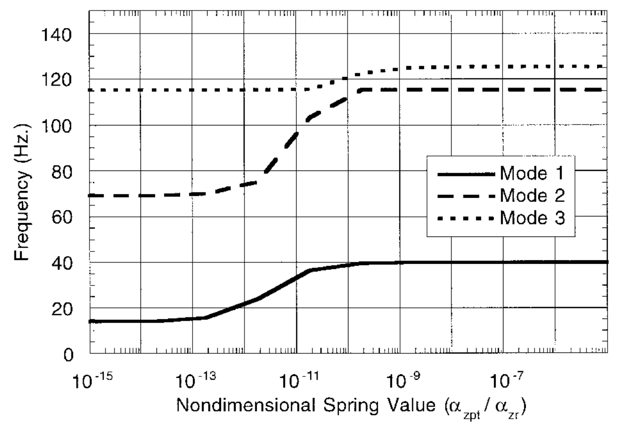

Fig. 8 Frequency in hertz as a function of nondimensional spring value for a symmetrically laminated $[30_2/0]_s$ cantilever plate having a point support at the corner intersection of the tip and trailing edges. The plate is made of glass/epoxy with plate geometry parameters as follows: β = 30, thickness = 0.14 in. (3.556 mm), aspect ratio = 3.11, taper ratio = 0.5, and area = 63.0 in.^{2} (406.45 cm^2).

Plates Having Elastically Restrained Point Supports

As mentioned earlier, the authors are interested in the application of the current method to the analysis of joined-wing and truss-braced aircraft. Figure 7 shows the convergence for the first three modes resulting from the number of terms in the series for a skew, symmetrically laminated $[30_2/0]_s$ cantilever plate, having a point support at the corner intersection of the tip and trailing edges. The plate is made of glass/epoxy with the properties E_1 = 38.61 GPa, $E_2 = E_3$ = 8.27 GPa, $G_{12} = G_{13}$ = 4.14 GPa, G_{23} = 3.35 GPa (calculated letting $G_{23} = 0.81G_{12}$), ν_{12} = 0.26, and ρ = 2546.54 kg/m^3. Plate geometry parameters are as follows: β = 30, thickness = 0.14 in. (3.556 mm), aspect ratio = 3.11, taper ratio = 0.5, and area = 63.0 in.^{2} (406.45 cm^2).

The same plate is then used to study the effect of changing the value for spring constant at the point support. Figure 8 shows the variation of the first three frequencies as a function of the point spring value nondimensionalized by the spring value used at the cantilevered edge that is applied to the transverse deflection. It can be seen that variations in the frequencies occur for α_{zpt}/α_{zr} between 10^{-14} and 10^{-7}. For values smaller and larger than this range, the solutions are obtained for the cantilevered plate without a point support and the cantilevered plate with a fixed point support, respectively. Appropriate choice of the elastically restrained spring value will permit the analysis of joined-wing and trussed-braced wing components.

Conclusions

Evaluation of the present method leads to several conclusions.

1) For plates with a relatively low number of elastically restrained or fixed point supports, the present method gives accurate results.

2) Elastically restrained points can effectively be included in the current plate model formulation. These can be used to investigate truss-braced wing and joined-wing configurations.

3) Using trial functions that satisfy the essential boundary conditions at the point supports may give better results for plates having many fixed point supports while using fewer terms than the present method using the Chebychev polynomials.

A simple and computationally efficient method has been developed for the study of thick, generally laminated plates having quadrilateral planform and arbitrarily located point supports. The method is ideal for procedures that require only the first few modes and having multiple calculations, such as in optimization. When multiple calculations are required, however, an eigenvalue extraction procedure such as the Lanczos method should be employed to efficiently calculate only the desired natural frequencies, i.e. first few modes. Because only the x and y locations of the point support are required to study the point support, it is trivial to move the support locations without the need for remeshing that may be necessary in a finite element approach. Therefore, the entire plate system is easily represented by design parameters such as span, aspect ratio, taper ratio, area, point support locations, and stacking sequence.

Numerous zeroth-order optimization methods exist that only require the function values, such as the simplex method, genetic algorithms, simulated annealing, etc., which can be used with the present method. Because the reverse transformation must be determined numerically, the derivatives of the stiffness matrix with respect to the point location values does not exist. However, if optimization methods requiring derivative information are used, the necessary derivatives can be generated using the response surface method. Thus, the present method can be utilized by numerous optimization methods.

Reference 20 identifies buckling of the tail section as a key constraint in the design of joined-wing aircraft. This is a separate design issue, and would have to be addressed by means other than the present method. However, the addition of buckling response using the current approach is currently being explored. Regardless, independent dynamic analysis of the wing and tail sections is possible with the present method, including flutter analysis. Additionally, because the joined wing response may be affected by rotational stiffness at the joint, rotational terms can easily be incorporated to the point support stiffness matrix, as mentioned earlier.

Including rib and spar contributions will lead to a better equivalent plate model for wing analysis, a procedure that is currently being developed. Applying the current approach for the elastically restrained points to the equivalent plate model will provide a more useful analysis tool for advanced-concept wings such as truss-braced wings and joined-wings.

Future work includes the addition of spring-supported masses located on the wing. These spring-supported masses can, for example, represent stores or engines attached to the wing. The present method was also applied to line-supported plates by using a large number of point supports to represent the line support. However, very poor convergence results were observed, indicating that more research needs to be performed before the method can be applied to line-supported plates. Because of this, the authors have developed a line-support formulation that shows reasonable results for the fundamental frequencies, but is still being investigated.[24]

Acknowledgments

The authors thank P. Mohan for providing the comparative finite element results for Table 6, using the three-node triangular finite element that was developed as part of his Ph.D. research work under the guidance of the senior author. Also, the authors thank D. MacMurdy for providing the modified reverse transformation subroutine for the current plate corner numbering scheme.

References

[1]Bhat, R. B., "Vibration of Rectangular Plates on Point and Line Supports Using Characteristic Orthogonal Polynomials in the Rayleigh-Ritz Method," *Journal of Sound and Vibration*, Vol. 149, No. 1, 1991, pp. 170–172.

[2]Gorman, D. J., "An Analytical Solution for the Free Vibration Analysis of Rectangular Plates Resting on Symmetrically Distributed Point Supports," *Journal of Sound and Vibration,* Vol. 79, No. 4, 1981, pp. 561–574.

[3]Gorman, D. J., "Free Vibration of Rectangular Plates with Symmetrically Distributed Point Supports Along the Edges," *Journal of Sound and Vibration*, Vol. 73, No. 4, 1980, pp. 563–574.

[4]Gorman, D. J., "A Note on the Free Vibration of Rectangular Plates Resting on Symmetrically Distributed Point Supports," *Journal of Sound and Vibration*, Vol. 131, No. 3, 1989, pp. 515–519.

[5]Raju, I. S., and Amba-Rao, C. L., "Free Vibrations of a Square Plate Symmetrically Supported at Four Points on the Diagonal," *Journal of Sound and Vibration*, Vol. 90, No. 2, 1983, pp. 291–297.

[6]Bapat, A. V., and Suryanarayan, S., "The Fictitious Foundation Approach to Vibration Analysis of Plates with Interior Point Supports," *Journal of Sound and Vibration*, Vol. 155, No. 2, 1992, pp. 325–341.

[7]Bapat, A. V., and Suryanarayan, S., "Free Vibrations of Periodically Point-Supported Rectangular Plates," *Journal of Sound and Vibration*, Vol. 132, No. 3, 1989, pp. 491–509.

[8]Bapat, A. V., and Suryanarayan, S., "Free Vibration of Rectangular Plates with Interior Point Supports," *Journal of Sound and Vibration*, Vol. 134, No. 2, 1989, pp. 291–313.

[9]Bapat, A. V., Venkatramani, N., and Suryanarayan, S., "A New Approach for the Representation of a Point Support in the Analysis of Plates," *Journal of Sound and Vibration*, Vol. 120, No. 1, 1988, pp. 107–125.

[10]Kerstens, J. G. M., Laura, P. A. A., Grossi, R. O., and Ercoli, L., "Vibrations of Rectangular Plates with Point Supports: Comparison of Results," *Journal of Sound and Vibration*, Vol. 89, No. 2, 1983, pp. 291–293.

[11]Narita, Y., "The Effect of Point Constraints on Transverse Vibration of Cantilever Plates," *Journal of Sound and Vibration*, Vol. 102, No. 3, 1985, pp. 305–313.

[12]Saliba, H. T., "Experimental Free Vibration Analysis of Rectangular Cantilever Plates with Rigid Point Supports," *Journal of Sound and Vibration*, Vol. 171, No. 4, 1994, pp. 459–472.

[13]Saliba, H. T., "Free Vibration Analysis of Rectangular Cantilever Plates with Symmetrically Distributed Point Supports Along the Edges," *Journal of Sound and Vibration*, Vol. 94, No. 3, 1984, pp. 381–395.

[14]Mizusawa, T., and Kajita, T., "Vibration of Skew Plates Resting on Point Supports," *Journal of Sound and Vibration*, Vol. 115, No. 2, 1987, pp. 243–251.

[15]Aksu, G., and Felemban, M. B., "Frequency Analysis of Corner Point Supported Mindlin Plates by a Finite Difference Energy Method," *Journal of Sound and Vibration*, Vol. 158, No. 3, 1992, pp. 531–544.

[16]Kitipornchai, S., Xiang, Y., and Liew, K. M., "Vibration Analysis of Corner Supported Mindlin Plates of Arbitrary Shape Using the Lagrange Multiplier Method," *Journal of Sound and Vibration*, Vol. 173, No. 4, 1994, pp. 457–470.

[17]Srinivasan, R. S., and Munaswamy, K., "Frequency Analysis of Skew Orthotropic Point Supported Plates," *Journal of Sound and Vibration*, Vol. 39, No. 2, 1975, pp. 207–216.

[18]Sadasiva Rao, Y. V. K., and Singh, G., "Vibration of Corner Supported Thick Composite Plates," *Journal of Sound and Vibration*, Vol. 111, No. 3, 1986, pp. 510–514.

[19]Gallman, J. W., and Kroo, I. M., "Structural Optimization for Joined-Wing Synthesis," *Journal of Aircraft*, Vol. 33, No. 1, 1996, pp. 214–223.

[20]Kroo, I. M., Gallman, J. W., and Smith, S., "Aerodynamic and Structural Studies of Joined-Wing Aircraft," *Journal of Aircraft*, Vol. 28, No. 1, 1991, pp. 74–81.

[21]Jobe, C. E., Kulfan, R. M., and Vachal, J. D., "Wing Planforms for Large Military Transports," AIAA Paper 78-1470, Aug. 1978.

[22]Lovejoy, A. E., and Kapania, R. K., "Natural Frequencies and an Atlas of Mode Shapes for Generally-Laminated, Thick, Skew, Trapezoidal Plates," Center for Composite Materials and Structures, Virginia Polytechnic Institute and State University, Rept. 94-09, Blacksburg, VA, Aug. 1994.

[23]Kapania, R. K., and Lovejoy, A. E., "Free Vibration of Thick Generally Laminated Cantilever Quadrilateral Plates," *AIAA Journal*, Vol. 34, No. 7, 1996, pp. 1474–1486.

[24]Lovejoy, A. E., and Kapania, R. K., "Free Vibration of Thick Generally Laminated Quadrilateral Plates with Point Supports," *AIAA/ASME/ASCE/AHS/ASC 37th Structures, Structural Dynamics, and Materials Conference and AIAA/ASME Adaptive Structures Forum*, Vol. 1, AIAA, Reston, VA, 1996, pp. 248–258.

[25]Murti, V., and Valliappan, S., "Numerical Inverse Isoparametric Mapping in Remeshing and Nodal Quantity Contouring," *Computers and Structures*, Vol. 22, No. 6, 1986, pp. 1011–1021.

[26]Kapania, R. K., and Mohan, P., "Static, Free Vibration and Thermal Analysis of Composite Plates and Shells Using a Flat Triangular Shell Element," *Computational Mechanics*, Vol. 17, No. 5, 1996, 343–357.